# The *Spitzer* Mid Infrared Proper Motions of the Cep E/HH 377 Outflow

A. Noriega-Crespo[1], A. C. Raga[2], A. Moro-Martìn[3], S. J. Carey[1] & N. Flagey[4]

[1] California Institute of Technology, [2] Centro de Ciencias Nucleares, UNAM, [3] Centro de Astrobiologia-INTA, [4] Jet Propulsion Laboratory, Caltech

## Abstract

We have used multiple epoch high angular resolution (~ 0.8") observations at 4.5 μm obtained with the Infrared Array Camera of the compact (~1.4') young stellar bipolar outflow Cep E to measure for first time in the mid-IR the proper motion of its brightest condensations. We found that for a distance of 730 pc, the tangential velocities of the North and South outflow are ~62 and 94 km/s respectively, and moving away from the central source roughly along the major axis of the flow. The emission at 4.5 μm is dominated by $H_2$ pure rotational lines, and therefore, confirms that the molecular Hydrogen gas moves at highly supersonic velocities, just like those of the ionic/atomic gas, without being dissociated. This strongly suggests either a very efficient mechanism in these objects to reform $H_2$ or the presence of strong magnetic fields to protect the molecular gas.

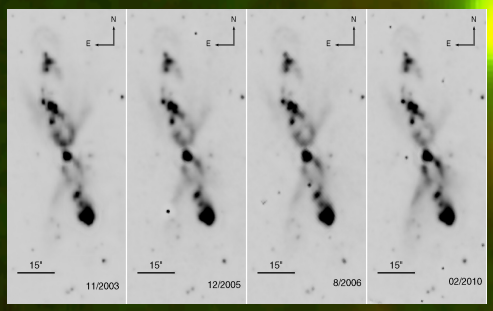


Fig 1. The multiple epochs of the IRAC 4.5um images of Cep E after reprocessing with the AWAIC HiRES software (60 iterations) that can reach an angular resolution of ~0.6-0.8".

## Introduction

The stability and longevity of the Infrared Array Camera (IRAC) on board the Spitzer Space Telescope is allowing experiments that were impossible to carry out before. The measurement of proper motions in the mid infrared of young proto-stellar outflows is one of them. We have recently shown that even at the relatively low angular resolution of IRAC (FWHM ~2"), in comparison with what is achievable with ground based telescopes in the visual or near infrared, it is possible to measure the proper motion of several outflows in the NGC 1333 region (Raga et al. 2012).

Proper motions (and the corresponding tangential velocities) are essential for determining the dynamics of the outflows, their momentum and energy transfer into the surrounding interstellar medium . The striking morphological similarity between the atomic/ionic gas emission (obtained from optical or near-IR observations) and that of the molecular Hydrogen (obtained either from near-IR or mid-IR observations), suggests that the kinematics of the proto-stellar outflows allow this relatively fragile molecule either to survive the shocks or to regenerate itself rapidly in the dense post-shock regions.

In this study we determine the proper motions of the deeply embedded and compact molecular outflow Cep E (Eislöffel et al. 1996; Ladd & Hodapp 1997; Noriega-Crespo, Garnavich & Molinari 1998; Moro-Martin et al 2001; Noriega-Crespo et al. 2004).

At a distance of ~730 pc, to measure proper motions within a time interval of ~6 yr (covered by the available IRAC images; Fig 1) is a considerable challenge, since velocities of ~100 km/s would correspond to shifts of only ~0.17". In order to achieve as high a resolution as possible, we have employed a high angular resolution enhancement of the IRAC images, reaching ~0.6"- 0.8" (Velusamy, Langer & Marsh 2007; Noriega-Crespo & Raga 2012; Velusamy et al. 2012). We include in the analysis two ground-based $H_2$ 2.12 μm images, with a 16 yr time interval (1996 & 2012), given the morphological similarity between the rotational and vibrational $H_2$ emission in Cep E.

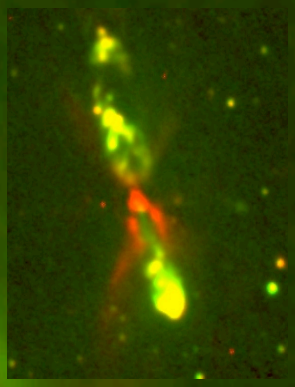

Fig 2. A two color image of the Cep E outflow combining IRAC 4.5 μm (red ) and $H_2$ continuum subtracted 2.12 μm(green).The morphology of the rotational and vibrational H2 emission is very similar, except that at 4.5 μm there is a cleraly scattered light from the outflow's cavity

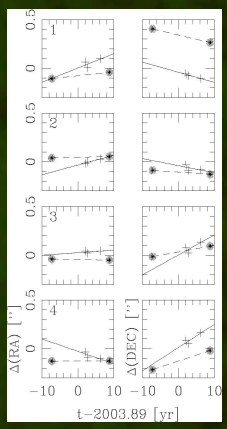


Fig 3. The positional changes in RA and DEC as a function of time for the four boxes along the Cep E outflow. The plus and star signs correspond to the 4.5 and 2.12 um emission, respectively. The overall proper motions are the same for both $H_2$ tracers.

## Proper Motions

We have defined four boxes, including the regions of convergence of the cavities and the bow-like structures, which we show in Figure 4. For each of these four boxes, we have carried out cross correlations between the emission in the 2003.89 frame and the other 4 available frames. From paraboloidal fits to the peak of cross correlation functions we then determine the offsets of the emission (within the four boxes, see Figure 4) with respect to the 2003.89 frame.

The resulting RA and DEC displacements are plotted as a function of time in Figure 3. From this Figure, we see that boxes 1 and 4 (corresponding to the bow-like structures) show substantial N-S motions, while the ``cavity tips" (boxes 2 and 3) have considerably lower proper motions. We have then carried out linear fits to the time dependencies of the RA and DEC offsets of our four boxes, from which we obtain the proper motions.

The resulting proper motion velocities are shown (together with their error boxes) in Figure 4. The bow-like structures show proper motions of ~62 km/s (Southern bow, box 1) and 94 km/s (Northern bow, box 4) directed approximately away from the outflow source. The Southern cavity tip (box 2) does not show a significant proper motion. The Northern cavity tip (box 3) shows a proper motion of 71 km/s at an angle of ~ 82º from the outflow direction (see Figure 4). This proper motion might reflect in part the significant intensity variations of the cavity emission during the observed time period (see Figure 1).

Fig 4. A false color image of Cep E outflow at 4.5μm showing the tangential velocities derived from the proper motions in the 4 selected boxes . Their magnitude and direction are consistent with those derived form the ionic/atomic gas.

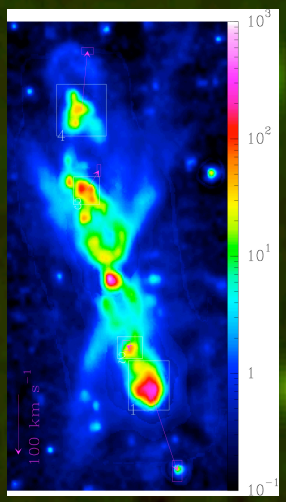


Cep E Proper Motions and Tangential Velocities from IRAC 4.5μm images[a]

| Box | $\Delta_x$ mas/yr | $\Delta_y$ mas/yr | $V_x$ km s$^{-1}$ | $V_y$ km s$^{-1}$ |
|---|---|---|---|---|
| 1 | 14.7±9.3 | -10.4±1.6 | 51.1±32.3 | -36.2±5.6 |
| 2 | 10.0±1.4 | -7.3±6.8 | 34.8±4.9 | -25.4±23.6 |
| 3 | 2.7±2.9 | 20.4±8.1 | 9.4±10.1 | 70.9±28.2 |
| 4 | -12.8±6.0 | 23.8±5.4 | -44.5±20.9 | 82.8±18.8 |

[a]For a distance of 730pc